PERGAMON

International Journal of Heat and Mass Transfer 43 (2000) 4175–4188

International Journal of HEAT and MASS TRANSFER

www.elsevier.com/locate/ijhmt

A non-equilibrium phenomenological theory of the mass and heat transfer in physical and chemical interactions Part II — modeling of the NH_3/H_2O bubble absorption, analytical study of absorption and experiments

M.D. Staicovici

Thermopower Equipment Research and Design Institute (SC ICPET — CERCETARE SA), 236 Vitan Road, 74369 Bucharest, Romania

Received 9 July 1998; received in revised form 10 January 2000

Abstract

A non-equilibrium phenomenological theory of mass and heat transfer, presented in previous works, is applied here in combination with the classical equilibrium phenomenological theory to model absorption of the ammonia bubble. The modeling tool is a non-empirical linear Phenomenological Hydro-Gaso-Dynamical (PhHGD) approach, outlined in the second section of this paper. First results refer to the elucidation of the problem of the ammonia bubble absorption, where from the following we are to be learned: (i) absorption process in the ammonia/water medium is a mass phenomenon and not a surface one; (ii) an *intensive* way of improving absorption is emphasized, which seeks to promote the i.p.a. effect appearance; this would replace the *extensive* way currently used, based on increasing gas–liquid interaction area; to this extent, the bubble absorber is hereby proposed for efficient absorption; (iii) the i.p.a. effect existence offers an additional chance for a satisfactory explanation of the Marangoni effect. The PhHGD code is extended to a refined analytical study of absorption, which may constitute a first data base for the bubble absorber. The paper also presents experimental results of ammonia bubble absorption in water, which are in good agreement with the predictions of the PhHGD approach.

1. Introduction

After periods of time of more or less intense utilization, the well-known NH_3/H_2O system has become a subject of topical interest again, owing to certain recent research work in the field of advanced thermal absorption (e.g. [3,6,21]) and to the new orientation towards applications, using natural working agents [16]. In this context, the correct evaluation of the NH_3/H_2O gas–liquid interactions plays an important role in the launching of this combination again.

Despite the comprehensive theoretical and practical experience in this system, the current assessment of the mass and heat transfer in NH_3/H_2O installations is made exclusively on a global scale and is based on empirical theories (e.g. of the two films, of penetration and renewal, [7]). A detailed experimental study of absorption in vertical pipe absorbers, made by Keizer [10], has demonstrated that the applicability of these theories to the NH_3/H_2O global system is questionable. He finally used empirical equations,

E-mail address: staicovici@dnt.ro (M.D. Staicovici).

0017-9310/00/$ - see front matter
PII: S0017-9310(00)00030-2

Nomenclature

C	local thermal capability (kJ/kmol), velocity of sound (m/s)
c_p	specific heat at constant pressure (kJ/kmol K)
d	injection nozzle diameter (m)
D_X	mass diffusivity coefficient (m^2/s)
D_T	heat diffusivity coefficient (m^2/s)
f	figure of merit quantifying the increase of a phenomenological function approaching an ideal state, as compared to its far equilibrium states
F_i	external force (N)
h	specific enthalpy (kJ/kmol)
i	specific mass current in the liquid (mol/sm^2)
j_r	reduced interface mass current
$j'_{i,\,g}$	interface mass current (mol/s)
$j''_{i,\,g,\,a}$	cumulated absorbed (interface) mass current, mol
$j'_{i,\,g,\,a,\,s}$	specific $j'_{i,\,g,\,a}$ or average absorption indicator (mol/s)
$j_{q,\,l,\,a}$	$j'_{i,\,g,\,a}$ coupled heat current (J)
$j''_{q,\,l,\,a,\,s}$	specific $j''_{q,\,l,\,a}$ (W)
$\dot{m}$, m	bubble feeding mass flow rate (kg/s)
n	number of bubbles
p	partial pressure (kPa, bar)
q	specific heat current in the liquid, coupled with i (W/m^2)
q, $\dot{q}_t$	tube feeding mass flow rate (kg/s)
r	radial coordinate (m)
R	bubble radius (m)
s	specific entropy (kJ/kmol K)
S	bubble area (m^2)
t	time (s)
T, t	temperature (K, °C)
v	liquid velocity (m)
V	bubble, tube volume (m^3)
x	liquid phase molar fraction (mol/mol)
y	gas phase molar fraction (mol/mol)
z	space coordinate (m)

Greek symbols

ρ	density, kg/m^3 ($kmol/m^3$)
σ	superficial tension (N/m)
σ'_{ik}	second order viscous tensor (N/m^2)
μ	chemical potential (kJ/kmol)
τ	bubble lifetime (s)
λ	thermal conductance (W/m K)
Δ	variation, duration

Subscripts

a	absorption, cumulated
b	bubble life time
e	equilibrium
i	mass
q	heat
g	gas, gaseous phase
l	liquid, liquid phase
s	specific
t	tube
0	initial

based on a Reynolds analogy, to correlate satisfactorily his experimental data.

To find a more accurate method for the evaluation of NH_3/H_2O gas–liquid interactions, Staicovici [25,26] proposes the use of a non-equilibrium phenomenological theory. It will be applied here in combination with the classical equilibrium phenomenological theory to model absorption of the ammonia bubble. The resulting modeling tool is a non-empirical linear Phenomenological Hydro-Gaso-Dynamical (PhHGD) approach. By doing so, an attempt is made to find an appropriate local solution of the transport in the NH_3/H_2O medium, which might lead to its correct global evaluation, applicable in the calculation of the absorption installation. Also, taking into account the findings of the author's previous works, there are additional good reasons to model the bubble absorption: (i) it is useful in explaining satisfactorily the ammonia bubble absorption problem [25,26]; (ii) it may contribute to a simpler experimental validation of the PhHGD method and (iii) from all interface shapes, the bubble quasi-spherical one, having highest (volume/area) ratio, promotes the best efficient absorption because it creates the best conditions for the i.p.a. effect appearance [25,26]. In the final part, starting from the bubble hydrodynamics, the paper presents the results of an analytic study of absorption, and gives experimental results obtained in bubble absorption and their comparison with those predicted by the modeling.

2. Application of the PhHGD approach to the bubble absorption

The PhHGD approach will be applied here, as a first attempt, to combine equilibrium and non-equilibrium phenomenological equations with classic hydro-gaso-dynamics, to assess an interface coupled

mass and heat transfer process, that of the bubble absorption. Solution of the problem at hand was faced from the very beginning with the following difficulties: (a) there are only a few papers in the specialized literature, which deal with a thorough analysis of bubble absorption/generation in multi-component media; (b) although the process is in evolution, none of the selected papers approach it with non-equilibrium phenomenological tools, all the authors preferring to consider a priori that an interface thermodynamical equilibrium exists, and (c) so far, the PhHGD method results may be only compared with experiment. The papers falling into the category mentioned above are due to Merrill and Perez-Blanco [17], who analyzed the bubble absorption in binary solutions, accompanied by combined mass and heat transfer and to Miyatake et al. [18], who give a simple universal equation for the bubble growth in pure liquids, and in solutions with non-volatile solute. Also, Sivagnanam [24] have developed correlations for the subcooled convection of binary mixtures during boiling, by using data for acetone–water, isopropanol–water and *n*-butanol–water, and Cooper and Stone [5] have reported experiments where vapor bubbles are grown on a flat wall in a binary liquid, which is initially stagnant and isothermal (hexane and octane in various proportions). Additionally, a lot of papers deal with the bubble dynamics in the context of boiling/condensation processes in pure liquids. For completion, some of them will be quoted hereinafter. Al-Hayes and Winterton [1] have obtained experimental results for the mass transfer in air bubbles adhering to the wall of a pipe in which the fluid (water, water with surfactants and ethylene glycol) has a supersaturated history. Nigmatulin et al. [20] examine a non-linear aspect of thermal and dynamic oscillating mass interaction, between a spherical vapor and gas bubble in a liquid, taking into account a non-uniform temperature in the bubble and the reciprocal diffusion in the gas–liquid mixture. Auracher and Maier [2] find a correlation for experimental data of vapor bubble condensation in slightly subcooled pure liquids (R11, R113, and C_3H_8O) governed by a heat transfer mechanism. Klausner et al. [11] determine the detachment time of vapor bubbles in forced convection boiling. In a two part paper, Zeng et al. [28] suggest a new model of prediction for the detachment diameters of vapor bubbles in the saturated stagnant liquid and in the flowing liquid upon boiling. Brujan [4] analyzes the question of the collapse of a spherical cavity bubble containing non-condensable gases and vapors in an infinite volume of non-Newtonian liquid. Lee and Merte [14,15] have examined the growth of the bubble in uniformly superheated liquids and under microgravity conditions.

The bubble evolution in the NH_3/H_2O gas–liquid interaction has been modeled in relation to the bubble generator scheme, shown in Fig. 1. This scheme represents a portion of a vertical pipe absorber. The gaseous mixture, coming from a reservoir of liquid NH_3/H_2O at pressure 1.2–1.5 bar and temperature 5–40°C, is expanded up to the value of the normal pressure and allowed to penetrate at flow rate $\dot{q}_t$ in a

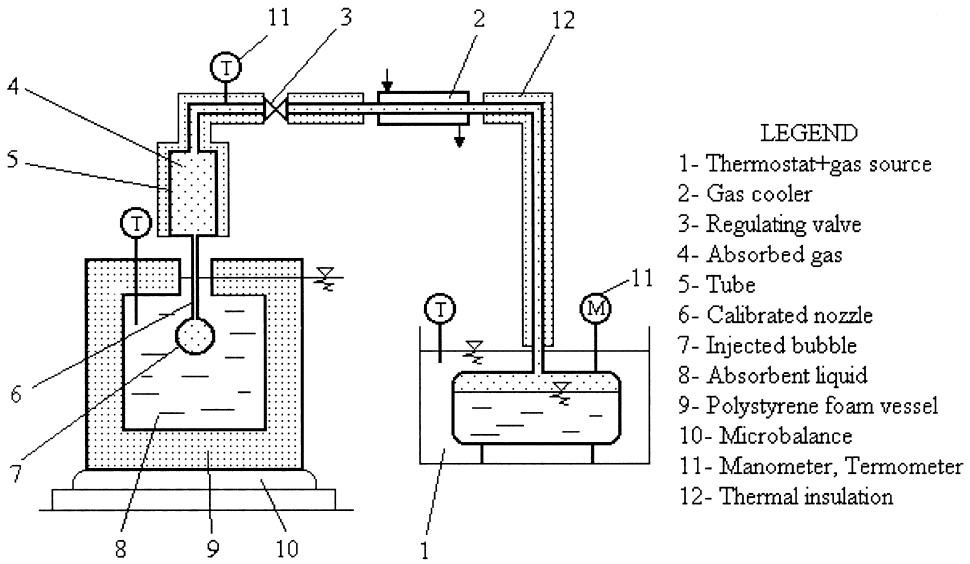

Fig. 1. Bubble generator scheme.

pressure-equalizing tube, which, in the case of vertical absorbers, has the role of a collector. The gas in the tube has pressure p_t, temperature T_g and volume V_t. From here, the gas passes through a calibrated nozzle and diameter d_0, and penetrates into the absorbing liquid mixture at the flow rate $\dot{m}$. The parameters of the gas injected in the liquid are p_g, T_g and y. At the gas–liquid interface and at infinity the liquid has the parameters p_l, T_l and x, respectively p_∞, T_∞, and x_∞.

2.1. Governing equations

Modeling is based upon the following assumptions, which are generally those formulated by Rayleigh [22] for the dynamics of a single bubble, namely a spherical symmetry flow and uniformity of the gas pressure in the bubble (homobaricity). When the bubble radius varies monotonously (growth or collapse), the homobaricity condition is written as [20] $(\dot{R}/C)^2 \ll 1$, where $\dot{R}$ and C are the bubble radius velocity, and the sound velocity in gas, respectively. During the bubble oscillations, homobaricity prevails if $\omega R \ll C$, where $\omega = 2\pi f$ is the annular frequency (f). Moreover, the following assumptions are considered for the liquid and gas medium: (a) the liquid gravitational forces are neglected; liquid is newtonian, viscous and incompressible; its physical and thermo-physical properties are constant in time (λ, c_p, ρ_l, σ, D_X); (b) the gas has an ideal behaviour and has an isothermal adiabatic evolution, both in the tube and in the bubble; the flow in the tube assumes negligible charge losses; the gas–liquid interaction is an evolutional phenomenon, deemed to be an open system from the thermodynamical point of view; the molar fraction as well as the specific heat at a constant pressure are constant.

2.1.1. Liquid phase equations

The liquid motion is governed by the following equations [13]

global continuity

$$\frac{\partial \rho}{\partial t} + \operatorname{div}\left(\rho \vec{v}\right) = 0 \tag{1}$$

continuity of a species

$$\rho \frac{\mathrm{d}x}{\mathrm{d}t} + \operatorname{div}\vec{i} = 0 \tag{2}$$

laminar flow (Navier–Stokes)

$$\rho \frac{\mathrm{d}\vec{v}}{\mathrm{d}t} = -\nabla p + \frac{\partial \sigma'_{ik}}{\partial z_k} + \sum F_i \tag{3}$$

general coupled mass and heat transfer (thermodiffusion)

$$\rho T \frac{\mathrm{d}s}{\mathrm{d}t} = \sigma'_{ik} \frac{\partial v_i}{\partial z_k} - \operatorname{div}\left(\vec{q} - \mu \vec{i}\right) - \vec{i} \nabla \mu \tag{4}$$

where [25]

$$\frac{\mathrm{d}s}{\mathrm{d}t} = c_p \frac{1}{T} \frac{\mathrm{d}T}{\mathrm{d}t} - \left(\frac{\partial \mu}{\partial T}\right)_{p,\,x} \frac{\mathrm{d}x}{\mathrm{d}t} \tag{5}$$

2.1.2. Interface equations

At interface, the equations governing interaction are the following:

motion

$$p_{l,\,r=R} = p_g - \frac{2\sigma}{R} + \rho_g (v_g - v_{r=R})\left(v_g - \dot{R}\right) \tag{6}$$

where v_g is the gas velocity, and $\dot{R} = \partial R/\partial t$;

gas mass balance

$$j_r \rho_l \dot{V} + \rho_g \left(v_g - \dot{R}\right) S = 0 \tag{7}$$

where S is the interface area, $\dot{V} = 4\pi R^2 \dot{R}$ is the time derivative of the bubble volume, and j_r is the reduced mass current involved in interaction [25,26]

liquid mass balance

$$j_r \rho_l |\dot{V}| + |v_{r=R}| \rho_l S = \rho_l |\dot{V}| \tag{8}$$

mass balance for a species

$$j_r \rho_l |\dot{V}| y + \rho_l |\dot{V}| (1 - j_r) x + \rho_l D_x \nabla x S = \rho_l |\dot{V}| (x + \delta x) \tag{9}$$

where δx is the actual increase of the molar fraction x.

energy

$$\rho_l |\dot{V}| c_{p,\,l} \delta T_l = j_r \rho_l |\dot{V}| C + \lambda \nabla T_l S \tag{10}$$

where δT_l is the actual increase of the liquid temperature at interface, and C is the local thermal capacity [26].

2.1.3. Gas phase equations

The gas phase is governed by the following equations:

law I of thermodynamics, for the gas in the tube

$$(\dot{q} - \dot{m}) h_g = \dot{p}_{g,\,t} V_t \tag{11}$$

where $\dot{q}, \dot{m}$ and V_t are the gas flow rate at which the tube is fed, the bubble and the tube volume, respectively.

Bernoulli equation (stationary), applied to the flow in the tube (the flow rate through the orifice, [9])

$$\dot{m} = \alpha\Omega\sqrt{\rho_g|p_{g,\,t} - p_g|} \tag{12}$$

where α is the Coriolis coefficient of the kinetic energy, and Ω is the nozzle flow section.
mass balance in the bubble

$$\dot{m} - j_r\rho_l|\dot{V}| = \rho_g\dot{V} \tag{13}$$

2.2. Model equations. Initial and boundary conditions

The governing equations will be written herein below in a form which allows for the application of the known mathematical methods of numerical solution. To this effect, we shall firstly revert to the liquid phase equation. A special analysis of the mass, $\vec{i}$, and heat, $\vec{q} - \mu\vec{i}$, flows in Eq. (4), derived from the entropy source equation of thermodiffusion, showed that off-diagonal effects Soret and Dufour are small in case of our application [25]. Hence, currents may not be coupled, resulting in pure diffusion

$$\vec{i} = -\rho D_X \nabla x \tag{14}$$

and pure conduction, respectively

$$\vec{q} - \mu\vec{i} = -\lambda\nabla T \tag{15}$$

The thermodiffusion equation is further simplified, noting that the terms $T(\partial\mu/\partial T)_{p,\,x}$ and $\vec{i}\nabla\mu$ may be neglected, as they are second-order terms, and the viscous tensor $\sigma'_{i,\,k}$ is canceled in the case of spherical symmetry contraction ($i = k$) and of the incompressible Newtonian liquid [13]. Equally, the integration of Eq. (1), written on spherical coordinates, leads to

$$r^2 v = R^2\dot{R} = \text{const} \tag{16}$$

where from

$$v = \dot{R}\left(\frac{R}{r}\right)^2 \tag{17}$$

At interface, from Eqs. (7) and (8) results in

$$\rho_g\left(v_g - \dot{R}\right) = -j_r\rho_l\dot{R} \tag{18}$$

and respectively

$$v_{r=R} = \dot{R}\left(\frac{R}{r}\right)^2(1 - j_r) \tag{19}$$

so that the equation of motion is re-written as

$$p_{l,\,r=R} = p_g - \frac{2\sigma}{R} + \left(j_r\rho_l\dot{R}\right)^2\left(\frac{1}{\rho_g} - \frac{1}{\rho_l}\right) \tag{20}$$

Finally, the flow equation (3) written on spherical coordinates and without the viscous term (see the remark above) is integrated in relation to the radial coordinate r, between R and ∞. Using Eq. (19), it results that

$$\left[\ddot{R}R + \dot{R}^2(1 + j_r)\right](1 - j_r) - \dot{R}R\frac{\partial j_r}{\partial t} = \frac{1}{\rho_l}(p_{l,\,r=R} - p_\infty) \tag{21}$$

The second term of the left side of the equation is a second-order term and may be neglected. Considering the above, modeling the bubble absorption/generation leads to the solving of the following system of non-linear ordinary differential equations and with partial derivatives [25,27]

$$\ddot{R} = \left[\left(p_{g,\,t} - \frac{\dot{m}^2}{\alpha^2\Omega^2\rho_g} - p_\infty - \frac{2\sigma}{R}\right)\frac{1}{\rho_l} + \dot{R}^2\left(j_r^2\frac{\rho_l}{\rho_g} - 1\right)\right]\frac{1}{R(1 - j_r)} \tag{22}$$

$$\dot{p}_{g,\,t} = \left[\dot{q}_t - \dot{m}\right]\frac{h_g}{V_t} \tag{23}$$

$$\frac{\partial x}{\partial t} + \dot{R}\left(\frac{R}{r}\right)^2\frac{\partial x}{\partial r} = D_X\left(\frac{2}{r}\frac{\partial x}{\partial r} + \frac{\partial^2 x}{\partial r^2}\right) \tag{24}$$

$$\frac{\partial T_l}{\partial t} + \dot{R}\left(\frac{R}{r}\right)^2\frac{\partial T_l}{\partial r} = D_T\left(\frac{2}{r}\frac{\partial T_l}{\partial r} + \frac{\partial^2 T_l}{\partial r^2}\right) \tag{25}$$

where

$$\dot{m} = \rho_g\dot{V} + j_r\rho_l|\dot{V}| \tag{26}$$

Eqs. (22)–(26) serve to determine the first four unknown factors, R, $p_{g,\,t}$, x and T_l, respectively. In the next step, the bubble radius velocity, $\dot{R}$, and the bubble radius acceleration, $\ddot{R}$, as well as the first time derivative of the gas pressure in the tube, $\dot{p}_{g,\,t}$, are determined. To determine the gas pressure in the bubble, p_g, and the liquid velocity, equations

$$p_g = p_{g,\,t} \pm \frac{\dot{m}^2}{\alpha^2\Omega^2\rho_g} \tag{27}$$

and, respectively, Eqs. (17) and (19) are used.

The initial and boundary conditions that ensure the uniqueness of the solution are as follows:

$t = 0; r \geq R$:

$$R(0) = R_0; \quad \dot{R}(0) = v_{r=R}(0) = 0; \quad T_l(0, r) = T_\infty;$$

$$x(0, r) = x_\infty$$

$$p_{g,\,t}(0) = p_\infty + \frac{2\sigma}{R_0} + \Delta p_{g,\,t_0}; \quad p_g(0) = p_\infty + \frac{2\sigma}{R_0};$$

$$p_l(0, r) = p_\infty$$

respectively,

$t > 0; r = R$:

$$\delta x = (y - x)j_r + D_X \frac{\nabla x}{|\dot{R}|}; \quad \delta T_l = \frac{1}{c_{p,\,l}}\left(j_r C + \frac{\lambda \nabla T_l}{\rho_l |\dot{R}|}\right)$$

$t \geq 0$:

$$p_l(t, \infty) = p_\infty; \quad T_l(t, \infty) = T_\infty; \quad x(t, \infty) = x_\infty$$

2.3. Numerical integration

The mathematical model presented in the previous section has been numerically integrated by means of a Runge–Kutta–Gauss code of solving non-linear ordinary differential equation systems applied to motion equations and by using an explicit scheme with finite differences for equations with partial derivatives. The forward time and the centered space have been used in the scheme with finite differences. The necessary thermodynamic factors (j_r, h_g, etc.) have been calculated at each time step by using the Ziegler and Trepp [30] state equation. To provide greater accuracy of the simulation, the mass diffusitivity coefficient, which is very important for the flow, has been adjusted at every time step according to the equation

$$D_X = (3x + 2)10^{-9} \tag{28}$$

(where the mass fraction x has a value calculated at the previous time step) without affecting the linearity of the equation with partial derivatives. Eq. (28) is valid within the range $0.0 \leq x \leq 0.7$ and has been determined by linear interpolation of the results obtained by Kojima and Kashiwagi [12].

2.4. Modeling results of the ammonia bubble absorption

Results have been obtained by means of a PhHGD computer code. Prior to start the computations we found the nearest ideal point which the system evolves, in order to calculate the match function $M(p_{r,\,e}, x_e)$ intervening in the force equation [26]. Normally, this should result from an iterative calculus, searching, according to a Prigogine theorem, the way of minimum entropy production. However, not all, but in many cases a simpler practical method can be considered, remarking that most systems have state parameters with quasi-constant values all along the evolution period, coming out of their connection with the infinite reservoirs or other engineering purposes etc. Depending on the system variance, these parameters partially or completely define the nearest ideal point. In our case, the ammonia/water system is biphase and bicomponent, so it suffices to have two such parameters, but the type of the parameters may change upon the specific application. For instance, for the absorption process of a closed system absorption refrigeration plant, these parameters are the rich solution final temperature, close to the sink source temperature and the absorbed gas molar fraction, but for the generation process, they change to the final poor solution temperature, close to the warm source temperature and the condensing pressure. In our case of the bubble absorption, the near ideal point is defined by the quasi-constant absorption pressure ($p_l = p_g$) and gas molar fraction y.

Absorption takes place between gas and the subcooled absorbent, when forces and currents are positive. The set of entry data corresponds to the absorption of the ammonia bubble ($y = 0.992$) in water ($x_\infty = 10^{-4}$), at normal pressure ($p_\infty = 1.001$ bar) and environment temperature ($T_\infty = 293$ K). The solution of the motion equation is shown in Fig. 2. Fig. 3 elucidates the problem of ammonia bubble absorption. Indeed, the reduced absorbed mass current j_r and the actual one

$$j'_{i,\,g} = j_r \rho_l |\dot{V}| \tag{29}$$

continuously increase during bubble growth time, causing the bubble pressure decrease, Fig. 4. At a certain moment, the actual current equals the bubble mass feeding rate m and the collapse starts. The cumulated absorbed mass current

$$j'_{i,\,g,\,a}(t) = \int_0^t j'_{i,\,g}(z)\,\mathrm{d}z \tag{30}$$

and the corresponding coupled heat current $j''_{q,\,l,\,a}$ are plotted against the bubble growth time in Fig. 5. The liquid mass fraction and temperature distributions are given in Figs. 6 and 7, respectively against same bubble growth time and the radial depth in liquid, measured from the interface. We note that liquid mass fraction and temperature almost linearly decrease with the radial depth during a complete evolution, and both ammonia and the thermal field diffuse over a distance of about 1.0×10^{-3} m.

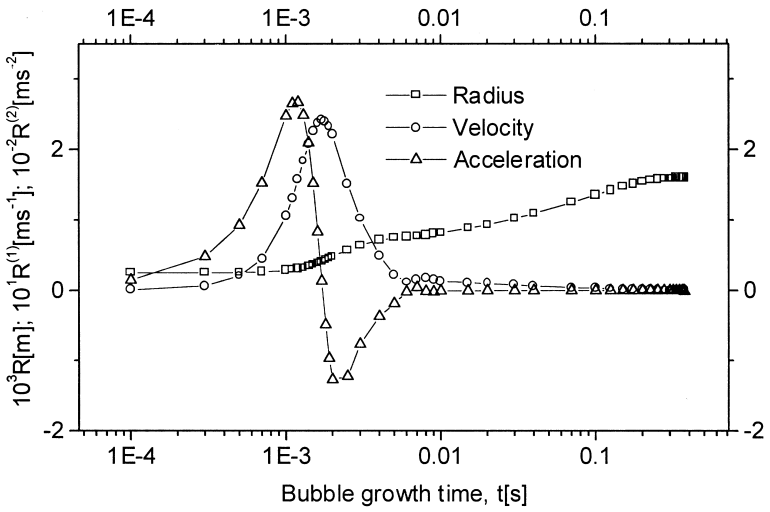

Fig. 2. Numerical solution of the dynamics of ammonia bubble absorption.

The phenomenological modeling of the bubble absorption may be a valuable lesson for a future advanced thermal absorption technology. Next, we synthesize what is to be learned from it. First, the *absorption process in ammonia/water medium is a mass phenomenon and not a surface one*, as pointed out also by Eq. (29). Second, absorption can be improved in an *intensive* way, seeking not the remoteness from the ideal point (see the classical point of view), but the nearness to it, when the currents naturally increase up to very high values without any additional technical improvements (see figure of merit $f = 740.7$ in Fig. 3, which is defined according to Staicovici [26]). The tendency manifested in the construction of NH_3/H_2O absorbers of increasing the gas–liquid contact area, through the dispersion of one of the phases to increase the absorption efficiency may not result in the anticipated effect. On the contrary, by extending the contact area the more rapid evolution of the interface towards the equilibrium parameters is delayed (the mass frac-

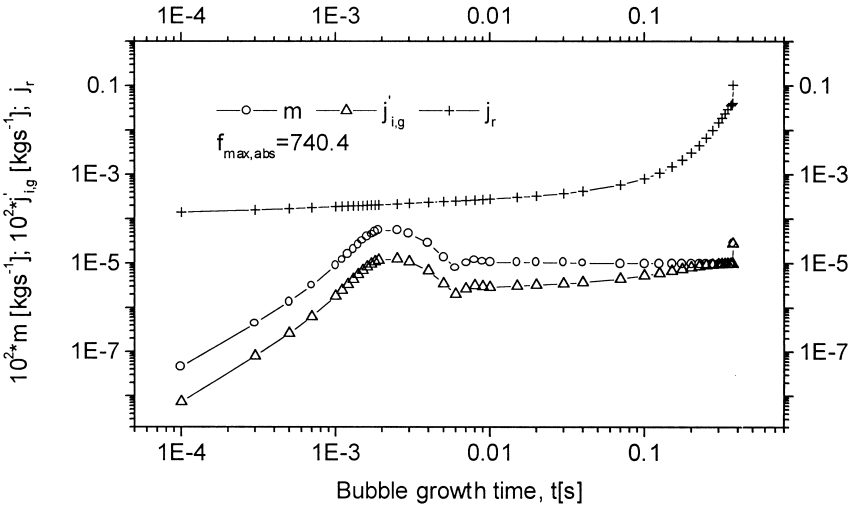

Fig. 3. Numerical phenomenological elucidation of the ammonia bubble absorption problem.

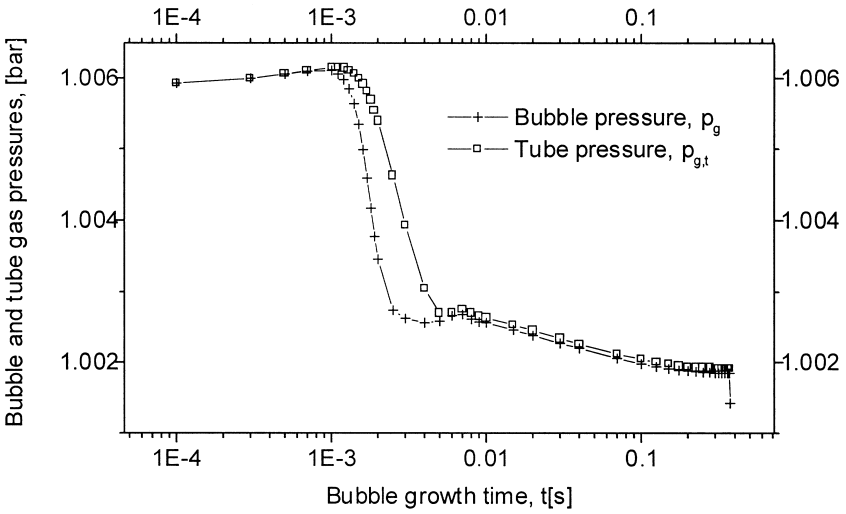

Fig. 4. Numerical solution of the tube and bubble pressure variation during ammonia bubble absorption.

tion x of the liquid at interface decreases with the increase of the contact area, at the same gas feeding flow rate) and absorption decreases, as compared to the one achieved in a less dispersed phase. Moreover, the auxiliary pumping energy consumption is also increased. Thus, in the light of the above, the increase of the contact area is merely an *extensive* technical solution, which helps to compensate the absorption decrease caused by an artificial remoteness from the ideal point, offering in exchange a more stable functioning of the absorbing device. In addition to the above, it is noted that quasi-spherical bubbles with a minimum contact area for the same volume, stands for the greatest chances to achieve the best mass and heat transfer through i.p.a. effect appearance. This gives rise to the idea of constructing a (NH_3/H_2O) bubble flow absorber [25]. It is a flat plate and is mounted horizontally. In comparison with a present (NH_3/H_2O) absorber with vertical pipes or with liquid phase dispersion, the bubble absorber offers the following advantages: (i) maximum absorption efficiency; (ii) minimum pressure loss on gas side; (iii) it is suited to a

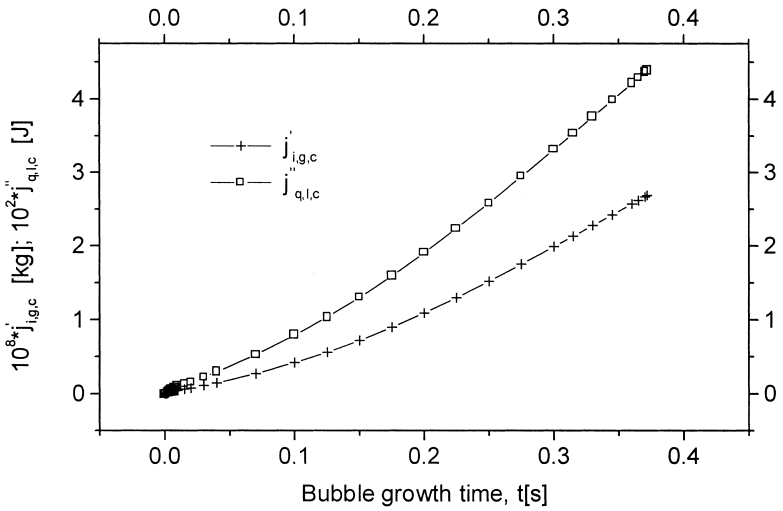

Fig. 5. Numerical solution of the cumulated absorbed mass and coupled heat currents during ammonia bubble absorption.

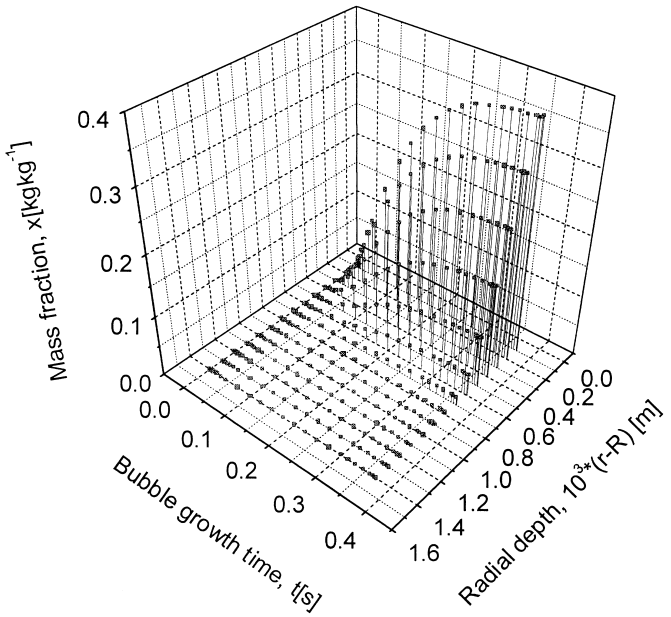

Fig. 6. Numerical solution of the liquid mass fraction evolution generated by the ammonia bubble absorption.

modern compact plate construction; (iv) minimum auxiliary energy consumption. Third, intensive theoretical and experimental research work has been carried out during the last decade aiming at improving absorption, by means of additives (surfactants) which stimulate the Marangoni convection [8,19,23]. Up to the present date there is no satisfactory explanation of the mechanism which generates this effect [29]. Most of the unsuccessful attempts have been based on the effect of superficial tension reduction in the liquid, obtained by means of additive agents. The non-equilibrium thermodynamics offers yet another chance to the clarification

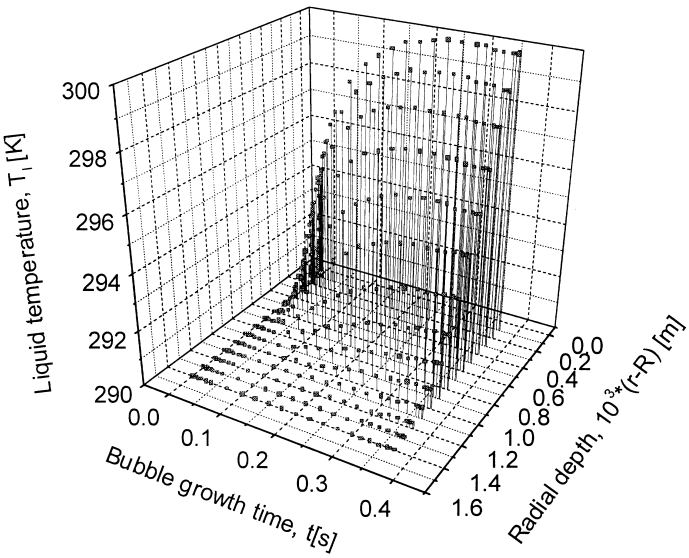

Fig. 7. Numerical solution of the liquid temperature evolution generated by the ammonia bubble absorption.

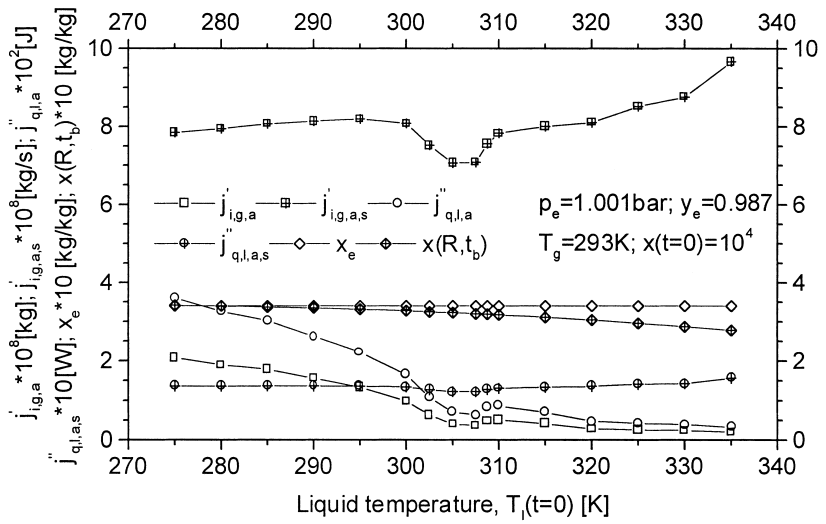

Fig. 8. Numerical study case of initial liquid temperature influence on mass and coupled heat currents in ammonia bubble absorption.

of this problem. Without having the intention to give a qualitative and so much more quantitative complete explanation, we will however make a primary analysis of the cause which can lead to the occurrence of the Marangoni effect from the non-equilibrium phenomenological point of view [25]. Here, contrary to the effect obtained by the dispersion of phases, by means of additive agents the interface area decreases considerably, and its parameters approach the equilibrium values. Interface becomes non-homogeneous, in the sense that violent absorption centers appear at its level, which alternate with weak interaction zones, due to the presence of the surfactant (which can be dissolved in the absorber or not). This non-homogeneity, influenced to a small extent by the superficial tension, causes an accentuated perturbation of the liquid surface, which is characteristic to Marangoni instability.

3. Analytical study of NH_3/H_2O absorption

The use of PhHGD code was extended to an ana-

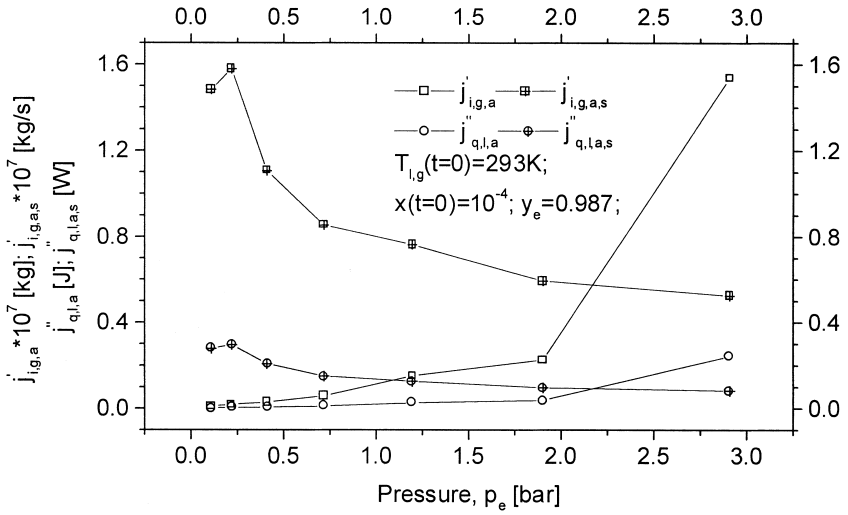

Fig. 9. Numerical study case of absorption pressure influence on mass and coupled heat currents in ammonia bubble absorption.

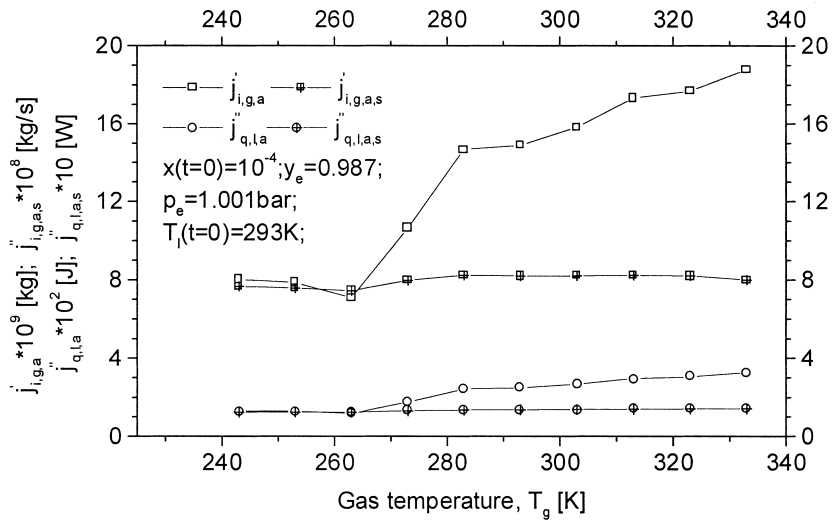

Fig. 10. Numerical study case of gas temperature influence on mass and coupled heat currents in ammonia bubble absorption.

lytical study of ammonia/water absorption [25]. The modeled scheme in Fig. 1 is not provided with a cooling system, absorption heat being naturally dissipated in the vessel with large heat capacity absorbent. Hence, from this point of view our results may differ to some extent to those which could be obtained on a better cooled absorber. However, they preserve the intrinsic important features of absorption, independent of the flow type, and constitute at the same time a first data base for the bubble absorber proposed in paragraph two. The absorption is appreciated by the cumulated absorbed mass current $j'_{i,\,g,\,a}$ and a specific $j'_{i,\,g,\,a,\,s}$, which is defined by the integral mean

$$j'_{i,\,g,\,a,\,s} = \frac{1}{\tau}\int_o^\tau j'_{i,\,g}(t)dt = \frac{1}{\tau}j'_{i,\,g,\,a}(\tau) \tag{31}$$

where τ is the bubble life time. The quantity expressed by Eq. (31) is a measure of absorption efficiency and is termed as average indicator of absorption. Addition-

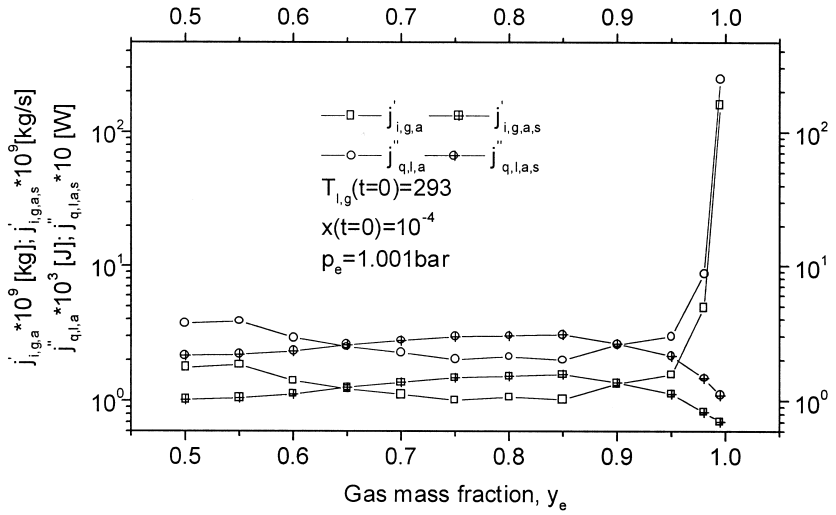

Fig. 11. Numerical study case of gas mass fraction influence on mass and coupled heat currents in ammonia bubble absorption.

ally, the results also include information about the coupled heat currents $j''_{q,\,l,\,a}$ and $j''_{q,\,l,\,a,\,s}$, defined similarly to theirs mass homologues. The results presentation is confined here only to show the influence on the absorption of the initial liquid temperature, absorption pressure, gas temperature and gas mass fraction, plotted in Figs. 8–11, respectively. Fig. 8 recommends that liquid initial temperature should not overcome to much the ideal point temperature, because the average absorption indicator decreases and its increase at higher temperatures is accompanied by important departures of liquid mass fraction x from the ideal value x_e. The absorption pressure shows considerable influence on absorption efficiency, the average indicator decreasing about three times when pressure increases from 0.2 to 2.9 bar, which is very surprising, Fig. 9. Working with as much as low absorption pressures is therefore desirable, but obviously this must also be correlated with the other design parameters of a plant. Fig. 10 shows little influence of the gas temperature on absorption. However, low gas temperatures should be avoided and on this purpose gas superheating, a common practice with absorption refrigeration plants, has from the mass/heat transfer point of view a second good reason. Fig. 11 shows a considerable influence which, this time, the gas mass fraction employed up on absorption efficiency. The cumulated absorbed mass current increases very much with y approaching unit. On the contrary, absorption efficiency decreases about twice from maximal values for same y variation, which is again very surprising. Bearing in mind its high energy consumption, vapor rectification, also commonly used in absorption plants, this time there is an additional reason to be avoided, that of decreasing mass/heat transfer in absorption processes. To this extent, on the opposite side, resorption plants gain twice eliminating rectification.

4. Experimental

Experiments of ammonia bubble ($y = 0.970$–0.991) absorption in distilled water ($x(t = 0) \leq 5.0 \times 10^{-4}$), at normal pressure ($p_l = p_g = 1.001$ bar) and temperatures of the gaseous and liquid phases of (5.1–19.4)°C and (1.2–17.0)°C, respectively, were accomplished. The testing scheme is given in Fig. 1. The temperatures of gas and liquid were measured by making use of 0.1°C precision thermometers. The tube feeding mass flow rate, $\dot{q}_t$, and the cumulated absorbed mass current $j'_{i,\,g,\,a}$ were gravimetrically estimated, with a microbalance (precision of 1.0×10^{-7} kg), weighting the mass of ammonia absorbed in the vessel containing the liquid absorbent during a timed period of time which corresponds to a pre-established number of injected bubbles. Time measurements were carried out by means of a chronometer with a precision 0.1 s. The gas mass fraction was assessed from readings of pressure and temperature of the ammonia/water solution contained in the reservoir and using current equilibrium data of ammonia/water combination. The mean experimental results are given in Table 1. For comparison, the same Table contains the cumulated absorbed mass currents calculated by means of the model given in Section 2 with experimental entry data. Although the experiments are in a reduced number for the moment, their good agreement, within ±15% confidence limits, with the modeling, validate the proposed combined non-equilibrium and equilibrium phenomenological approach for mass and heat transfer local processes in ammonia/water mixtures.

5. Conclusions

Despite the comprehensive theoretical and practical experience in the NH_3/H_2O system, the current assessment of the mass and heat transfer in installations working with it is made exclusively on a global scale and is based on empirical theories (e.g. of the two films, of penetration and renewal). According to a detailed study of absorption, the applicability of these theories here is questionable. Today, the common practice for this assessment is to use the experiment and the Reynolds analogy correlations, although this technique is confronted with limited predictive qualities. To find a more accurate method for the evaluation of NH_3/H_2O gas–liquid interactions, a non-equilibrium phenomenological theory is applied in this work in combination with the classic equilibrium phenomenological theory and the hydro-gaso-dynamics to model absorption of the ammonia bubble. The resulting modeling tool is a non-empirical linear (PhHGD) approach. First results refer to the elucidation of the problem of the ammonia bubble absorption, where the followings are to be learned from:

1. absorption process in the ammonia/water medium is a mass phenomenon and not a surface one;
2. an intensive way of improving absorption is emphasized, which seeks to promote the i.p.a. effect appearance; this would replace the extensive way currently used, based on increasing gas–liquid interaction area; to this extent, the bubble absorber is hereby proposed for efficient absorption;
3. the i.p.a. effect existence offers an additional chance for a satisfactory explanation of the Marangoni effect.

The PhHGD code is extended to a refined analytical study of absorption, which may constitute a first data base for the bubble absorber. The paper also presents experimental results of ammonia bubble absorption in

Table 1
Experimental/model comparison for $j'_{i,\,g,\,a}$ in ammonia/water bubble absorption tests[a]

	Mean experimental								Model	$j'_{i,\,g,\,a}$ relative error (%)
Run no.	T_g ($\pm$0.05°C)	$T_l(t=0)$ ($\pm$ 0.05 °C)	$10^3 y$ ($\pm$0.5)	n	$\Delta t \pm 0.05$ (s)	$10^6 \Delta m \pm 5 \times 10^{-8}$ (kg)	$10^{10} q (= \frac{\Delta m}{\Delta t})$ (kg/s)	$10^{10} j'_{i,\,g,\,a} (= \frac{\Delta m}{n})$	$10^{10} j'_{i,\,g,\,a}$	
1	12.9	1.20	980	40	36.3	1.80	496 ± 14.5	450 ± 12.5	453 ± 11.2	± 5.3
2	19.0	2.40	970	40	30.0	1.10	367 ± 17.3	275 ± 12.5	278 ± 13.5	$+8.2$ -10.4
3	18.5	3.20	988	40	20.5	1.78	867 ± 26.5	447 ± 12.5	278 ± 12.0	$+9.5$ -2.1
4	17.9	4.75	991	40	26.7	1.70	637 ± 19.9	425 ± 12.5	394 ± 14.2	$+14.9$ -0.8
5	17.5	6.50	987	40	24.2	1.43	593 ± 21.9	358 ± 12.5	331 ± 12.1	$+15.9$ -0.4
6	19.2	7.70	983	20	14.6	0.83	572 ± 36.2	417 ± 25.0	404 ± 23.2	$+15.3$ -8.9
7	19.4	9.80	991	20	8.4	0.85	995 ± 65.5	425 ± 25.0	436 ± 26.3	$+9.1$ -14.1
8	5.1	11.70	991	40	20.9	1.92	919 ± 26.1	450 ± 12.5	442 ± 11.0	$+7.2$ -3.6
9	18.9	13.9	989	40	15.2	1.37	903 ± 35.9	342 ± 12.5	321 ± 13.3	$+14.9$ -1.8
10	18.6	14.8	987	40	15.1	1.21	805 ± 35.8	303 ± 12.5	308 ± 12.1	$+6.3$ -9.5
11	18.4	16.6	985	40	18.5	1.22	659 ± 28.8	304 ± 12.5	292 ± 14.3	$+13.5$ -5.3
12	18.3	17.0	987	40	16.5	1.25	760 ± 32.6	312 ± 12.5	329 ± 12.2	$+2.1$ -12.5

[a] ($p_l = p_g = 1.001; x(t=0) < 4.8 \times 10^{-4}; \sigma = 6.0 \times 10^{-2}; \lambda = 0.5; R_0 = d = 2.5 \times 10^{-4}; V_t = 4.0 \times 10^{-6}$).

water, which are within ±15% confidence limits with the predictions of the PhHGD approach. This first successful example shows that the two phenomenological approaches, non-equilibrium and equilibrium, lead to same results and can be coupled in order to assess coupled mass and heat transfer at least for the local processes at hand.

Acknowledgements

The author thanks professor M.D. Cazacu at the Polytechnical University of Bucharest for the valuable assistance in performing the crude material of this two part paper.

References

[1] R.A.M. Al-Hayes, R.H.S. Winterton, Bubble growth in flowing liquids, Int. J. Heat Mass Transfer 24 (1981) 213–221.
[2] H. Auracher, M. Maier, Vapor bubble condensation in slightly subcooled pure liquids, in: 16th Int. Congr. Refrigeration, B1, 1983, pp. 269–274.
[3] J. Bassols, R. Schneider, First results of the operation of a gas-fired 250 kW absorption heat pump, Heat Pumps for Energy Efficiency and Environmental Progress (1993) 447–452.
[4] E.A. Brujan, Heat transfer in spherical bubble dynamics, Conf. Hydraulic Machinery and Hydrodynamics, Timisoara 2 (1994) 103–110.
[5] M.G. Cooper, C.R. Stone, Boiling of binary mixtures — study of individual bubbles, Int. J. Heat Mass Transfer 24 (12) (1981) 1937–1950.
[6] D.C. Erickson, Branched GAX absorption vapor compressor, US Patent 5097676, 1992.
[7] T. Hobler, Mass Transfer and Absorbers, Pergamon Press, Oxford, 1966.
[8] L. Hoffman, I. Greiter, A. Wagner, V. Weiss, G. Alefeld, Experimental investigation of heat transfer in a horizontal tube falling film absorber with aqueous solutions of LiBr with and without surfactants, Int. J. Refrig. 19 (5) (1996) 331–341.
[9] D. Ionescu, Introduction to Hydraulics (in Romanian), Technical Publishing House, Bucharest, 1977.
[10] C. Keizer, Absorption refrigeration machines, Ph.D. Thesis, Department of Mechanical Engineering, Delft University of Technology, Delft, 1982.
[11] I.F. Klausner, R. Mei, D.M. Bernhard, L.Z. Zeng, Vapor bubble departure in forced convection boiling, Int. J. Heat Mass Transfer 36 (3) (1993) 651–662.
[12] M. Kojima, T. Kashiwagi, Mass diffusivity measurements for ammonia–vapor absorption processes, in: 19th Int. Congr. of Refrigeration, Hague, IV(a), 1995, pp. 53–360.
[13] L. Landau, E. Lifchitz, Mécanique des fluides, Mir, Moscow, 1971.
[14] Ho Sung Lee, Herman Merte Jr., Spherical vapor bubble growth in uniformly superheated liquids, Int. J. Heat Mass Transfer 39 (12) (1996) 2427–2447.
[15] Ho Sung Lee, Herman Merte Jr., Hemispherical vapor bubble growth in microgravity: experiments and model, Int. J. Heat Mass Transfer 39 (12) (1996) 2449–2461.
[16] G. Lorentzen, The use of natural refrigerants: a complete solution to the CFC/HCFC predicament, Int. J. Refrig. 18 (3) (1995) 190–197.
[17] T.L. Merrill, H. Perez-Blanco, Combined heat and mass transfer during bubble absorption in binary solutions, Int. J. Heat Mass Transfer 40 (3) (1997) 589–603.
[18] Osamu Miyatake, Itsuo Tanaka, Noam Lior, A simple universal equation for bubble growth in pure liquids and binary solutions with a nonvolatile solute, Int. J. Heat Mass Transfer 40 (7) (1997) 1557–1584.
[19] R. Möller, K.F. Lnoche, Surfactants with NH_3–H_2O, Int. J. Refrig. 19 (5) (1996) 317–321.
[20] R.I. Nigmatulin, N.S. Khabeev, F.B. Nagiev, Dynamics, heat and mass transfer of vapor–gas bubbles in a liquid, Int. J. Heat Mass Transfer 24 (6) (1981) 1033–1044.
[21] M.V. Rame, D.C. Erickson, Advanced absorption cycle: vapor exchange GAX, in: Int. Abs. Heat Pump Conf., AES-31, ASME, 1993, pp. 25–32.
[22] Lord Rayleigh, On the pressure developed in a liquid during the collapse of a spherical cavity, Phil. Mag. 34 (1917) 94–98.
[23] D. Rie, T. Kashiwagi, Computer simulation of vapor–absorption enhancement into H_2O/LiBr absorbed by Marangoni convection, JSME Int. J. II 34 (1991) 355–361.
[24] P. Sivagnanam, A.R. Balakrishnan, Y.B.G. Varma, On the mechanism of subcooled flow boiling of binary mixtures, Int. J. Heat Mass Transfer 37 (4) (1994) 681–689.
[25] M.D. Staicovici, Contributions to two-phase flows and heat transfer in solar refrigerating installations (in Romanian), Ph.D. Thesis, Bucharest Polytechnics University, 1998.
[26] M.D. Staicovici, A non-equilibrium phenomenological theory of the mass and heat transfer in physical and chemical interactions Part I — application to NH_3/H_2O and other working systems, Int. J. Heat Mass Transfer (1998).
[27] M.D. Staicovici, Numerical phenomenological approach of transport provided biphase flow for NH_3/H_2O absorption/generation elementary processes (in Romanian), in: Proc. Eighth National Conference of Thermopower, Pitesti, 29–30 May, II, 1998, pp. 269–280.
[28] L.Z. Zeng, J.F. Klausner, D.M. Bernhard, R. Mei, A unified model for the prediction of bubble detachment diameters in boiling systems — II. Flow boiling, Int. J. Heat Mass Transfer 36 (9) (1993) 2271–2279.
[29] F. Ziegler, G. Grossman, Heat-transfer enhancement by additives, Int. J. Refrig. 19 (5) (1996) 301–309.
[30] B. Ziegler, C. Trepp, Equation of state for ammonia–water mixtures, Int. J. Refrig. 7 (1984) 101–106.